

SPECTRAL AND THERMAL ANALYSIS STUDY OF SOME TRANSITION METAL COMPLEXES DERIVED FROM BIS(2,2'-METHYLYLIDENE PHENOL)DIAMINOETHANE.

DOI: 10.25177/JCCMM.2.1.2

Research

AUTHOR: Nworie Felix Sunday

July 2017

Copy rights: © This is an Open access article distributed under the terms of Creative Commons Attribution 4. 0 International License.

Received Date: 08th June 2017Accepted Date: 20th July 2017Published Date: 15th Aug 2017

NWORIE, F.S and NWABUE, F.I
DEPARTMENT OF INDUSTRIAL CHEMISTRY, EBONYI STATE UNIVERSITY, PMB 053 ABAKALIKI, EBONYI STATE, NIGERIA.

CORRESPONDING AUTHOR:

Nworie Felix Sunday
Email: nworie.felix@gmail.com

CONFLICTS OF INTEREST

There are no conflicts of interest for any of the authors.

ABSTRACT

The thermodynamics of complexation and thermal properties of mixed ionic complexes of the types $M(H_2L)X_2$ and $M(HL)X$ (where $M = Fe(II), Fe(III), Co(III), Ni(II),$ and $Cu(II)$., $L = bis(2,2'$ -methylidene phenol) diaminoethane, and $X =$ anions of the types $Cl^-, NO_3^-, SO_4^{2-}, ClO_4^-$ or OH^-) prepared using extractive method have been investigated. Thermal decomposition of the transition metal complexes took place in two or three distinct steps in exothermic reaction up to $800^\circ C$. The heat capacity change (ΔC_p), transition midpoint temperature (T_m), entropy change (ΔS_m°), calorimetric enthalpy (ΔH_m°), Gibbs free energy change ($\Delta G^\circ(T)$), denaturation enthalpy ($\Delta H^\circ(T)$) and denaturation entropy ($\Delta S^\circ(T)$) were calculated from the results of differential scanning calorimetry (DSC) while Vant Hoff thermodynamic properties was used to calculate the stability constants of the complexes in solution. It was found that the stability constants of the complexes follow the order $Fe(II) > Fe(III) > Cu(II) > Ni(II) > Co(II)$ while the denaturation enthalpy and entropy of the complexes follow the order $Ni(II) > Fe(II) > Fe(III) > Co(II) > Cu(II)$ respectively.

KEYWORDS: bis(2,2'-methylidene phenol) diaminoethane, transition metal complexes, thermal analysis, thermodynamic parameters.

INTRODUCTION

The development of the field of inorganic and physical chemistry has increased in recent years with increased synergy especially in the area of Schiff bases and their transition metal complexes. Bis(2,2'-methylidene phenol) diaminoethane its derivatives and transition metal complexes have played significant role in bioinorganic chemistry and applications [1-2] in catalysis and in electrocatalytic reactions [3-5], as oxidizing agent [6-7], as nanocomposite and nanoparticles [8-9], as corrosion inhibitor [10], in carbon capture for purifying the environment [11], as red phosphorescent light emitting diode (Ph OLEDs) [12] and as metallomesogens [13].

Even though some authors [14-16] have incriminated some Schiff bases and their metal complexes as potential antimicrobial agent, none have related the thermodynamic stability and denaturation enthalpy and entropy to the biochemical nature of the synthesized metal complexes. Similarly some authors [12,17-18] who worked on H_2L and complexes only concentrated on melting point determination and thermal stability without indepth treatment of the thermodynamic properties. Again, most studies concentrated on complexes of H_2L prepared using constituent combination method [19] but this work was on the thermal and thermodynamic properties of

H₂L complexes prepared using extractive techniques. In this work, spectral, thermodynamic and thermal methods were applied in the characterization of H₂L transition metal complexes which are very important in bioinorganic chemistry and applications.

2.0 MATERIALS AND METHODS

2.1 Reagents and equipment.

Analytical grade reagents (Merck, Germany) were used without further purification unless otherwise mentioned. All aqueous solutions were prepared in distilled water and working solutions prepared by dilution as required. Bis(2,2'-methylidene phenol) diaminoethane(H₂L) shown in figure I was prepared as reported elsewhere [20]. Stock solutions of Fe(II), Fe(III), Co(II), Ni(II) and Cu(II) were prepared using (NH₄)₂SO₄.FeSO₄.6H₂O, Fe₂(SO₄)₃.9H₂O, CoCl₂.6H₂O, NiSO₄.7H₂O and CuSO₄.5H₂O (Merck, Analar grade). Stock solutions of mineral acids (HCl, HNO₃ and H₂SO₄) were prepared by diluting the concentrated acids and were standardized using appropriate standard bases.

Electronic spectra of the ligand and complexes in chloroform solution were obtained on Jenway Uv – Vis spectrophotometer model 6105. DSC analysis (Thermal degradation pattern) was determined using NETZSCH DTA 404PC Differential scanning calorimeter. Metal-ligand mole ratio was determined using jobs method of continuous variation as described elsewhere [21]. Microanalysis of the ligand and complexes were done at the Department of Chemistry, Rhodes University, South Africa.

2.2. Synthesis of metal complexes

An aliquot of a sample solution containing 100µg each of Fe(II), Fe(III), Cu(II), Ni(II) and Co(II) was transferred into a 20 mL calibrated extraction bottle and volume was made up to 5 mL with acid solution of concentration 0.0001M. This was followed with the addition of 0.5mL of ligand solution. 5 minutes for colour development was allowed and complexes formed extracted with 5 mL chloroform. The organic extracts were allowed to dry and product recrystallized using carbon tetrachloride, dried and characterized (M.P >250⁰C for Fe(II) while for Fe(III), Cu(II), Ni(II) and Co(II) M.P >300⁰C).

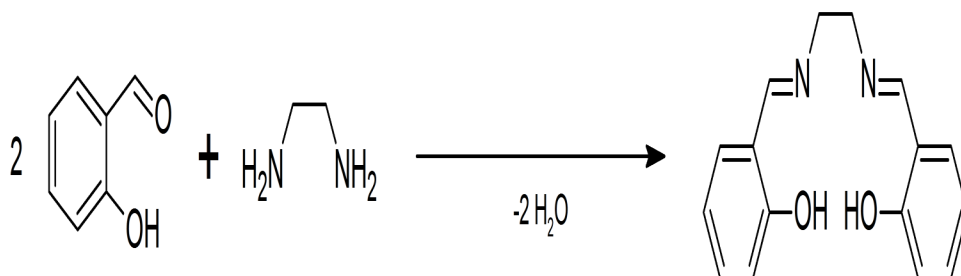


Figure 1: Synthesis of the ligand H₂L

2.3 Thermal Analysis Using Differential Scanning Calorimeter

The sample and reference pan were placed at separate furnaces maintained by separate heaters. Both sample and reference were maintained at same temperature and the difference in thermal power required maintaining them at the same temperature measured and plotted as a function of temperature or time. Differential heat flow was due to heat capacity associated with heating the sample. Small samples (5.00 mg) were weighed into an alumina crucible and mass noted. The crucible was covered with its cover usually slightly smaller. The TA Blue DSC sample press was used to close the crucible. The enclosed sample was placed side by side with the empty alumina crucible as reference. The instrument was purged with ultra pure N₂ gas at regulated pressure between 100 and 140 Kpa guage (15 and 20 Psi). The gas flow rate was set at 50 mL per min and experiment run from room temperature to 800 ⁰C at scan rate of 10 ⁰C min.

3.0 RESULTS AND DISCUSSION

3.1 UV-Vis Data and metal-ligand mole ratio.

Electronic spectrum of the Ni(II)H₂BMPDE complex exhibited three bands in the region 24691cm⁻¹ assignable to $1A_{1g} \rightarrow 1T_{2g}$ and 33898 and 38462 cm⁻¹ due to charge transfer transitions respectively notable in square planar environment for Ni(II) ion [22]. The absence of bands around 10120-11605, 16062-16180 and 25210 - 25575cm⁻¹ assignable to, $3A_{2g}(F) \rightarrow 3T_{2g}(F)$, $3A_{2g}(F) \rightarrow 3T_{1g}$ and $3A_{2g}(F) \rightarrow 3T_{1g}(P)$ respectively are due to charge transfer transitions from ligand to Ni(II) ion [23-25].

The electronic spectrum of cobalt (II) oxidized to Co(III) complex a d^6 ion consists of three bands in the region 25000, 29851 and 38462 cm^{-1} . The appearance of the band in the region 25000 cm^{-1} assignable to $4A_{2g} \rightarrow 2T_{1g}(F)$ indicated distorted octahedral geometry around the cobalt(II) ion whereas the band in the region 29851 and 38462 cm^{-1} are due to charge transfer transitions [26-27]. Similarly the broad band region of the electronic spectra of Co^{3+} a d^6 covering the long wavelength region 335-400 nm was assigned to an octahedral $3A_{2g} \rightarrow 2T_{1g}(P)$ transition [28].

For Cu^{2+} ion a d^9 , a band displayed in the electronic spectrum in the region of 28571 cm^{-1} characteristic of $2B_{1g} \rightarrow 2E_g$ transitions was typical of a distorted octahedral geometry. The $2E_g$ and $2B_{1g}$ states of d^9 octahedral copper (II) ion splits up under the influence of octahedral field (tetragonal distortion). The distortion can cause three transitions $2B_{1g} \rightarrow 2A_{1g}$, $2B_{1g} \rightarrow 2B_{2g}$ and $2B_{1g} \rightarrow 2E_g$ typical of distorted octahedral geometry [29]. The electronic spectra of Fe^{3+} H_2BMPDE a d^5 ion consist of three bands in the region of 43478, 37037 and 23529 cm^{-1} . The band at 23529 cm^{-1} assignable to $6A_{1g} \rightarrow 4T_{2g}(G)$ suggested distorted octahedral geometry [30-31]. The other band 43478 and 37037 cm^{-1} are due to charge transfer transition [26,31]. The electronic spectra of Fe^{2+} H_2BMPDE a d^6 ion consists of three bands in the region 30762, 40000 and 47619 cm^{-1} . The band at 30769 cm^{-1} was assigned to $4A_{2g} \rightarrow 2T_{1g}(F)$ indicating distorted octahedral geometry of Fe(II) ion (El-Gamel, 2012). The band at 40000 and 47619 cm^{-1} are due to charge transfer transitions [22]. The metal-ligand mole ratio as determined from jobs plot indicated 1:1 stoichiometry for all the transition metal complexes and similar observations have been made [32] with related derivatives.

3.2 Thermodynamics of Complexation

The Vant Hoff thermodynamic properties of H_2L and HL complexes are shown in table I. Entropy and enthalpy changes were positive for all the complexes. The stability constants of the complexes increased in the order $\text{Fe(II)} > \text{Fe(III)} > \text{Cu(II)} > \text{Ni(II)} > \text{Co(II)}$.

The complexation process increased as temperature increased for all the metal ions until at a maximum of about 35 °C. The increased complexation of the metal ions to the ligand at relatively high temperatures (between 20-35 °C) showed that the complexation process may be endothermic [33]. From table II, Gibb's free energy change values were found to be negative indicating the feasibility and spontaneity of the complexation. The positive sign of enthalpy change confirmed that the complexation process was endothermic. The negative value of entropy change showed that the complexation involved solvation process [34]. Similarly the values of stability constants indicated that iron (II) and iron (III) metal ion complexes are more stable than others [34]. The thermodynamic parameters of complexation such as enthalpy (ΔH^0), entropy (ΔS^0), Gibb's free energy (ΔG^0) and stability constant (β_n) are listed in table I and are calculated from the variation of the thermodynamic equilibrium constant, K_0 at different temperatures as shown in equation 1.

$$K_0 = \frac{C_1}{C_2} \dots\dots\dots 1$$

C_1 is the amount of metal ion complexed per unit mass of ligand and C_2 the concentration of metal ion in the aqueous phase [33].

The standard enthalpy change of complexation (ΔH^0), the standard entropy change of complexation (ΔS^0), Gibb's free energy of complexation (ΔG^0) and stability constant for complexation (β_n) were calculated as shown in equation 2, 3 and 4.

$$\ln K_0 = \frac{\Delta S^0}{R} - \frac{\Delta H^0}{RT} \text{ (Vant Hoff plot) } \dots\dots\dots 2$$

$$\Delta G^0 = -RT \ln K_0 \dots\dots\dots 3$$

$$\Delta G^0 = -2.303RT \beta_n \dots\dots\dots 4$$

Thus, T represents the temperature in K while R is the universal gas constant ($\text{KJ Mol}^{-1}\text{k}^{-1}$). The thermodynamic values are given in Table 2.

AUTHOR: Nworie Felix Sunday							
Metal complexed	com-plexed	T(K)	lnK ₀	βn	ΔG (KJ Mol ⁻¹)	ΔH (KJ Mol ⁻¹)	ΔS(KJ Mol ⁻¹ K ⁻¹)
Fe(III)	288	4.59	1.813	-10.99	20187.85	-52.406	
	293	2.43	1.055	-5.919			
	298	0.559	0.243	-1.385			
	303	0.198	0.086	-0.498			
Fe(II)	288	4.18	1.814	-10.00	5462.11	-65.63	
	293	4.056	1.76	-9.88			
	293	3.94	1.71	-9.76			
	303	3.17	1.38	-7.98			
	308	3.112	1.35	-7.96			
	313	2.94	1.27	-7.65			
Ni(II)	288	3.17	1.38	-7.59	1155.74	-0.1817	
	293	3.10	1.35	-7.55			
	293	3.00	1.30	-7.55			
	303	2.90	1.26	-7.43			
	308	2.923	1.27	-7.48			
	313	2.923	1.27	-7.60			
Co(II)	288	2.495	1.08	-5.97	14680.49	-47.51	
	293	2.429	1.05	-5.97			
	293	2.31	0.985	-5.62			
	303	0	-0	0			
Cu(II)	288	3.66	1.59	-8.76	7654.36	-22.50	
	293	3.47	1.506	-8.45			
	293	2.99	1.298	-7.41			
	303	2.09	0.906	-5.26			
	308	2.034	0.8817	-5.20			
	313	1.967	0.854	-5.12			

Table 1 : Vant Hoff Thermodynamic Parameters of H₂L and HL complexes

Legend:T=temperature, $\Delta S = \text{entropy change}, \Delta H = \text{enthalpy change}, \beta n = \text{stability constant}, \Delta G^0 = \text{Gibb's free energy}.$

3.4 Kinetics of complexation

The kinetics of complexation of metal ions to the ligand (H₂L) at different contact time (1, 3, 5, 10 and 15 minutes) and at constant ligand and acid concentration of 0.5 % and 10⁻⁴ M respectively was performed. Contact time of 10,5,10, 10 and 5 mins was sufficient to achieve equilibrium for iron (III), iron(II), cobalt(II), nickel(II) and copper(II) metal ions complexation with H₂L ligand respectively. The commonly used kinetic models were applied on the complexation data the Lagergren pseudo-first –order model and pseudo-second –order shown in equations 5 and 6 respectively.

$$\ln(q_e - qt) = \ln q_e - k_1 t \dots\dots\dots 5$$

$$t/qt = 1/K_2 q_e^2 + t/q_e \dots\dots\dots 6$$

q_e is the amount of metal ion complexed with ligand at equilibrium (μg) and q_t is the amount (μg) of metal complexed at time t (min) whereas K₁ and K₂ are rate constants of pseudo-first order and second –order models respectively. A linear plot of ln(q_e-q_t) versus t for Pseudo-first –order model and t/q_t versus t for second –order –model clearly described the relevance of the models with the slopes as K₁ and K₂ respectively. Based on the high regression coefficient of the metal ions complexation on the ligand as shown from the pseudo-second –order kinetic model (R²=0.9984, 0.9993, 0.9948, 0.9983,0.9994 for iron(II), iron (III), cobalt(II), nickel(II) and copper(II) respectively in relation with pseudo-first –order kinetic model (R²=0.6634, 0.6102, 0.3382, 0.383 and 0.6118 for iron(II), iron (III), cobalt(II), nickel(II) and copper(II) respectively), the complexation was best described by the Pseudo –second –order kinetic model.

3.5 DSC studies

Metal complex	T	T _m	ΔH_m°	ΔCp	ΔS_m°	$\Delta G^{\circ}(T)$	$\Delta H^{\circ}(T)$	$\Delta S^{\circ}(T)$	
Fe ³⁺ HL	317.7	302.1	235	34.1	0.778	-0.034	766.96	2.49	
	425.4	405.2	138.4	34.9	0.342	-0.178	843.38	2.04	
	783.6	776.9	880.2	8.6	1.13	2.103	937.82	1.20	
Fe ²⁺ HL	109.2	98.1	-49.62	23.9	-0.506	0.019	220.45	2.055	
	290	275.4	536.2	40.9	1.95	-0.83	1133.3	4.06	
	811.1	802.4	108.6	18.9	0.135	0.276	273.03	0.338	
Ni ²⁺ HL	146.4	141.4	31.24	13.7	0.221	-0.009	99.74	0.697	
	509.2	496.1	-101.8	19.4	-0.205	-0.099	152.34	0.300	
	617.6	573.1	576.7	55.5	1.006	0.161	3046.4	5.156	
	842.2	836.6	444.66	14.1	0.531	0.365	523.56	0.623	
Co ²⁺ H ₂ L	117.8	124.8	-181.3	12.8	-1.45	-0.34	270.9	0.711	
	519.2	505.6	234	29.1	0.46	1.424	513.36	1.23	
	626.3	601.6	106.1	31.1	0.176	0.218	874.27	1.427	
	667.3	695.4	269	34.5	0.387	0.119	700.45	-1.036	
Cu ²⁺ H ₂ L	345.6	332.3	166.9	19.6	0.502	0.085	427.58	1.27	
	539.1	545.2	10.7	8.8	0.019	0.341	-42.98	-0.08	
	623.2	619.6	54.81	37.4	0.088	0.285	189.45	0.304	
	792.2	802.7	36.8	51.1	0.046	-0.124	-499.75	-0.626	

Table 2 : Thermodynamic Data on the DSC Decomposition of H₂L and HL Complexes.

T(°C)=Temperature, T_m(°C) = Transition midpoint temperature, ΔH_m° (J/K) = calorimetric enthalpy, ΔCp (°C) = change in heat capacity, ΔS_m° (J/K) = entropy change, $\Delta G^{\circ}(T)$ = free energy change, $\Delta S^{\circ}(T)$ = denaturation entropy, $\Delta H^{\circ}(T)$ = denaturation enthalpy.

The DSC curve for Fe²⁺HL, Cu²⁺HL, Co²⁺H₂L, Fe³⁺HL and Ni²⁺HL was subdivided into two, three, three, two and three main exothermic stages respectively as shown in table II. The thermal degradation patterns could have been due to loss of hydroxyl group, loss of component attached to the phenolic moiety, ligand degradation or decomposition and final decomposition to metal oxide. For Fe^{II} HL, the weak endothermic peak at 98.1 °C corresponds to morphological transformation or loss of hydroxyl group or smaller fragment [35] while the sharp endothermic peak at 275.4 °C corresponds to the melting point of the complex. This was followed by a strong exothermic peak at 802.4 °C corresponding to the decomposition of the complex. For Cu²⁺ HL, the DSC thermogram showed single sharp endothermic peak at 332.3 °C corresponding to the melting point of the complex. This was followed by three exothermic peaks at 545.2, 619.6 and 802.7 °C corresponding to the stepwise decomposition of the complex. The DSC curve of Fe³⁺ HL showed three peaks, one of the peaks corresponds to endothermic process while two corresponds to exothermic processes. The sharp endothermic peak at 302.1 °C corresponds to the melting point of the complex whereas the broad peaks at 405.2 °C and 776.9 °C corresponds to stepwise decomposition of the complex. The DSC curve of Ni²⁺ HL showed four peaks, 141.4 °C, 496.1 °C, 573.1 °C and 836.6 °C. The first weak endothermic peak (141.4 °C) corresponds to morphological transformation while the second sharp endothermic peak 496.1 °C corresponds to the melting point of the complex. The last two peaks at 573.1 °C and 836.6 °C corresponds to stepwise decomposition of the complex. The DSC curve of Co²⁺ H₂L showed four peaks. The first weak endothermic peak at 124.8 °C corresponds to morphological transformation while the second sharp endothermic peak 505.6 °C corresponds to melting point of the complex. The last two broad exothermic peaks at 601.6 °C and 695.4 °C correspond to stepwise decomposition of the complex.

Calculations from DSC data as shown in table II, presented negative values of ΔS at some steps indicating the reactions are slower than expected thereby establishing nonspontaneous nature of the reaction. Positive value

of ΔG in some steps supports the nonspontaneous nature of the degradation process [36]. Similarly, the positive value of enthalpy indicated the endothermic nature of the degradation process [37].

The calorimetric enthalpy (ΔH_m^0) values indicated that the transition is highly co-operative as denaturation occurs within narrow range of temperature [37-38]. Based on the results, degree of denaturation entropy and denaturation enthalpy of the H₂L complexes increased from Ni²⁺ → Fe²⁺ → Fe³⁺ → Co²⁺ → Cu²⁺.

The values of ΔS_m^0 was derived from the relation in equation 7

$$\Delta S_m^0 = \Delta H_m^0 / T_m \dots\dots\dots 7$$

$\Delta G^0(T)$ was calculated from the modified Gibb's Helmotz equation (Bruylants *et al.*, 2005) as shown in equation 8

$$\Delta G^0(T) = \Delta H_m^0 \left(1 - \frac{T}{T_m}\right) + \Delta Cp[(T - T_m) - T \ln\left(\frac{T}{T_m}\right)] \dots\dots\dots 8$$

The denaturation entropies and enthalpies $\Delta S^0(T)$ and $\Delta H^0(T)$ respectively were derived from Kirchoff's laws [38] as shown in equations 9 and 10.

$$\Delta H^0(T) = \Delta H_m^0 + \Delta Cp(T - T_m) \dots\dots\dots 9$$

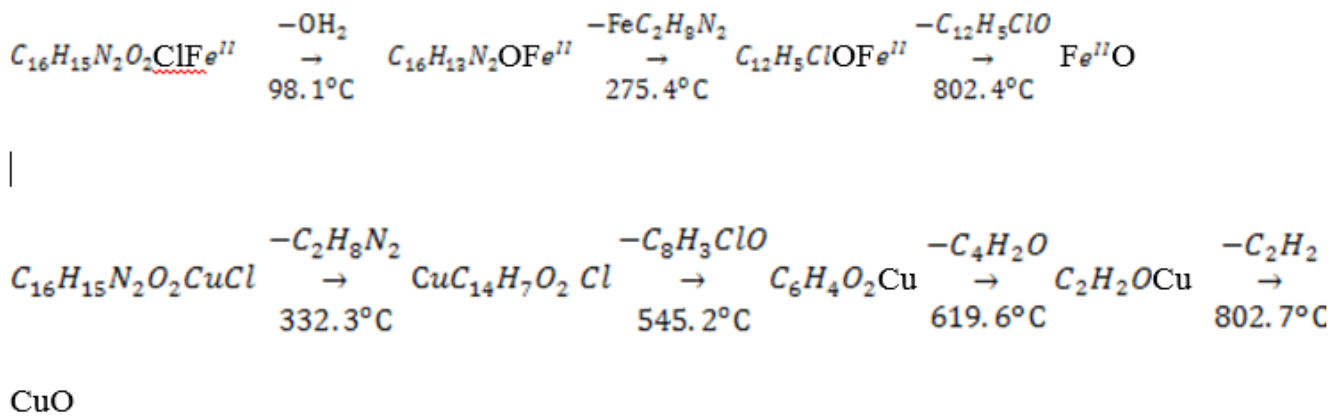
$$\Delta S^0(T) = \Delta S_m^0 + \Delta Cp \ln\left(\frac{T}{T_m}\right) \dots\dots\dots 10$$

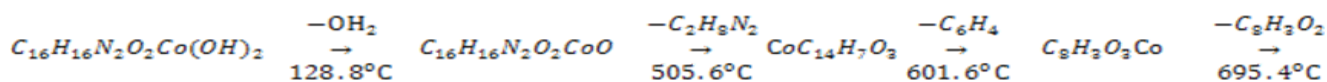
The stabilities of the complexes were determined using the free energy change ($\Delta G^0(T)$) which was the overall contribution of the enthalpic and entropic terms evaluated using calorimetric method.

Differential scanning calorimetry studies on the complexes showed the stages of decomposition of the complexes with temperature variation. The thermal degradation patterns have been attributed to loss of water, loss of component attached to the phenolic moiety, ligand degradation or decomposition and final decomposition to metal oxide. Similar observations have been seen in complexes of bis(salicylaldehyde)ethylenediamine [39]. The proposed thermal degradation pattern of the complexes are illustrated in fig 2.

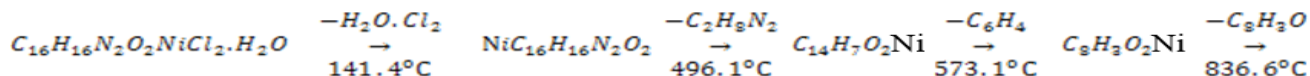
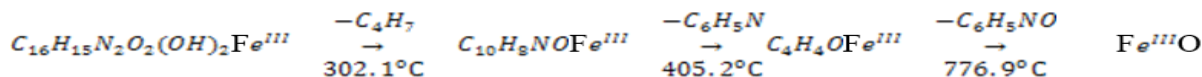
CONCLUSION

In conclusion, the thermal properties of the complexes of H₂L synthesized using extractive technique have been critically studied. The complexation which indicated formation of mixed ionic complexes was nonspontaneous and the DSC decomposition of the complexes have shown their degrees of biochemical stability.





CoO



NiO

Figure 2 : Proposed degradation pattern of H₂L and HL complexes.

REFERENCES:

1. Woldemarian G A , Mandal S S . Iron(III) salen Damages DNA and Induces Apoptosis in Human Cell Via. *J. Inorg. Biochem.* 2008;102: 740-7.
2. Rosas-Garcia VM, Martinez PE, Rodriguez N P, Martinez BN. Potential Oxygen –Carrying Complexes by Design. *Quimica Hoy Chemistry Sciences.* 2012; 2(4): 30-3.
3. Sonkar P K, Ganesan V, Rao V. Electrocatalytic Oxidation and Determination of Cysteine at Oxovanadium(IV) salen Coated Electrodes. *Int. Journal of Electrochemistry.* 2014; 1-6.
4. Katsuki T .. Functionalization of Metallosalen Complexes: Diverse Catalytic Performances and High Asymmetry Inducing Ability. *Chem Lett,* 2006; 124:1-12.
5. Zhang W, Loebach JL, Wilson SR, Jacobsen EN. Enantioselective Epoxidation of Unfunctionalized Olefins Catalyzed by (Salen) Manganese Complexes. *J. Am. Chem. Soc.* 1990; 112: 2801-3.
6. Perumal S, Thangadurai V, Thiruthimuthu K, Chandra R S. Role of Iron (III)- Salen Chloride as Oxidizing Agent with Thiodiglycolic Acid: The Effect of Axial Ligands. *J. Mex. Chem. Soc.* 2004;58(2): 211-17.
7. Alioke C U, Ukoha P O, Ukwueze N N, Ujam O T, Asegbeloyin J N. Kinetics and Mechanism of the Reduction of N,N¹-salicylideneiminatoiron(III) Complex Ion by L-ascorbic acid in Aqueous Acid Medium. *Chemistry and Materials Research.* 2012;2(7):48-57.
8. Du J, Cheng F, Wang S, Zhang T, Chen J. M(salen)-Derived Nitrogen Doped M/C (M=Fe, Co, Ni) Porous Nanocomposites for Electrocatalytic Oxygen Reduction. *Scientific Reports (4386) Conference Proceedings AP Energy* 2014; 4: 1-7.
9. Zhu Z, Wang S, Du J, Jin Q, Zhang T, Cheng F, Chen J. Ultrasmall Sn Nanoparticle Embedded in Nitrogen – Doped Porous Carbon as High Performance Anode for Lithium-ion Batteries. *Nano Lett.* 2014; 14(1):153-7.
10. Murugaiyan M, Madhu P, Vennila P ,Venkatesh Investigation of Schiff Base N, N¹ –bis (Salicylidene)- 1,2-Diaminoethene(salen) as Corrosion Inhibitor for Mild Steel in H₃P₀₄ Solution. *International journal of Chem Tech Research.* 2014/2015; 7(5): 2489-98
11. Starkie C.. Advances in Carbon Capture and Storage Research. *John Matthey Technol. Rev* 2015; 59(3): 182-187.
12. Bae HJ, Hwang KY, Lee M H, Do Y. Salen-Aluminium Complexes as Host Materials for Red Phosphorescent Organic Light Emitting Diodes. *Bull. Korean. Chem. Soc.* 2011; 32(9): 3290-94.
13. Abe Y, Nakabayashi K., Matsukawa N, Takashima H, Lida M, Tanase T, Sugibayashi M, Mukai H, Ohta K.. Chain Formation via the VO Units in the Liquid Crystal. *Inorg. Chin. Acta.* 2006; 359(12): 3934-46.
14. Doctrow SR, Huffman K, Marcus CB, Tocco G, Malfroy E, Adinolfi, C A, Kruk H, Baker K, Lazarowych N, Mascarenhas J, Malfroy B. Salen Manganese Complexes as Catalytic Scavengers of Hydrogen Peroxide and Cytoprotective Agents: Structure- Activity Relationship Studies. *J. Med. Chem.* 2002;45: 4549
15. Doctrow S R, Liesa M, Melov S, Shirihai OS, Tofilon P. Salen Mn Complexes are Superoxide Dismutase/ Catalase Mimetics that Protect the Mitochondria. *Curr. Inorg. Chem.* 2012; 2: 325-334
16. Johnson C, Long B, Ngugen JG, Day V W, Borovi AS, Subramaniam B, Guzman J. Correlation Between Active Centre Structure and Enhanced Dioxygen Binding in Co(salen) Nanoparticles: Characterization by In Situ Infrared, Raman, and X-ray Absorption Spectroscopies. *J. phy. Chem. C.* 2008; 112(32) :12272-81
17. Kumar D N, Garg BS. Some New Cobalt(II) Complexes: Synthesis, Characterization and Thermal Studies. *Jour-*

- nal of Thermal Analysis and Calorimetry*. 2002; 6(2):607-16.
18. Al-hamadani UJ , Abid DS. Synthesis of Iron(III) Complex of Polyester and Study of its Liquid Crystalline and Catalytic Properties. *Journal of Basrah Researchers (sciences)*. 2011;37(3A):100-103
 19. Cozzi PG. Metal –salen Schiff Base Complexes in Catalysis. Practical Aspects. *Chem. Soc. Rev.* 2004; 33: 410-21.
 20. Nworie FS , Nwabue FI. Solvent Extraction Studies of Metal Complexes Derived from a Tetradentate Schiff Base Bis(salicylidene)ethylenediamine (H₂SAL) in Acid Medium. *International Journal of Innovative and Applied Research*. 2014; 2 (6): 66-75.
 21. Nwabue F I, Okafo E N .Studies on the Extraction and Spectrophotometric Determination of Ni(II), Fe(II), Fe(III) and V (IV) with Bis (4-hydroxypent-2-ylidene) Diaminoethane. *Talanta*. 1991; 39(3): 273-280.
 22. Boghaei DM, Lashanizadega M. Template Synthesis Characterization of Highly Unsymmetrical Tetradentate Schiff Base Complexes of Nickel(II) and Copper(II). *J.Sci.I.R. Iran*. 2000; 2: 301.
 23. Rathore K, Singh RK, Singh HB. Structural, Spectroscopic and Biological Aspects of O, N Donor Schiff Base Ligand and its Cr(III), Co(II) Ni(II) and Cu(II) Complexes Synthesized through Green Chemical Approach. *E-Journal of Chemistry*. 2010; 7: 5566-72.
 24. Ukoha PO, Oruma US. Synthesis and Antimicrobial Studies of N,N¹-bis(4-dimethylaminobenzylaldehyde) ethane-1,2-diamine and its Nickel(II) and platinum(IV) Complexes. *Journal Chem Soc. Nigeria*. 2014; 39(2):102-7.
 25. Zahid H L, Syed KAS. Spectral, Magnetic and Biological Studies on Some Bivalent 3d Metal Complexes of Hydrazine Derived Schiff –Base Ligands. *Metal –Based Drugs*. 1997; 4(2): 65-8.
 26. Yang S, Kwon H, Wang H, Chang K, Wang J. Efficient Electrolyte of N, N¹-bis(salicylidene) ethylenediamine zinc(II) Iodide in Dye-sensitized Solar Cells. *New. J. Chem*. 2010; 34, 313-7.
 27. Singh K, Baruwa MS, Tyagi P. Synthesis, Characterization and biological activities of Co(II), Ni(II), Cu(II) and Zn(II) Complexes with Bidentate Schiff Bases Derived by Heterocyclic Ketone. *Eur Journ Medicinal Chem*. 2006; 41 (1) :147 -153.
 28. Prakash A, Pal Ganwar M, Singh KK . Synthesis, Spectroscopy and Biological Studies of Ni(II) Complexes with Tetradentate Schiff Bases having N₂O₂ Donor Group. *J. Dev. Biol. Tissue Eng* . 2011;3(2): 13-19.
 29. El-Gamel N E A, Zayed MA. Fluoroquinolone Antibiotic (Enrofloxacin) Metal Complexes. Synthesis, Spectroscopic and In vitro Antimicrobial Screening Properties. *World Journal of pharmaceutical research*, 2014;4 (1):142-62.
 30. El-Gamel NEA .Co-ordination Behavior and Biopotency of Metal N, N- Salen Complexes. *RSC Advances*, 2012; 2:5870-6.
 31. El-Gamel NEA, Zayed MA. Synthesis, Structural Characterization and Antimicrobial Activity Evaluation of Metal Complexes of Sparfloxacin. *Spectrochim Acta*, 2011; 82:414-23.
 32. Lloret F, Moratal J, Faus J. Hydrolytic Decomposition of Salen in Acid Solution: Solution Chemistry of N,N¹-ethylenebis(salicylideneiminato)Iron(III). *International Journal of Inorganic and Organometallic Chemistry*. 1983; 10: 1743-8
 33. El- Binda A- A, El- sonbati, M A D, Abd – El kader M K Potentiometric and Thermodynamic Studies of Some Schiff Base Derivative of 4- Aminoantipyriane and their Metal Complexes. *Journal of Chemistry*. 2013. 68218: 1-6
 34. Samir A A, Saber EM, Abdulrahman, A F Potentiometric, Spectrophotometric, Conductimetric and Thermodynamic Studies on Some Transition Metal Complexes Derived from 3—methyl-1-phenyl- and 1,3,- diphenyl- 4—aryazo- 5- pyrazolones. *Nature and science*. 2010; 2 : 793- 803.
 35. Lee CH, Hsu CK, Chang CL. A Study on the Thermal Decomposition Behaviours of PETN, RDX, HNS and HMX, *Thermochim. Acta*. 2002; 173: 392-3
 36. Borah D, Baruah M K. Kinetic and Thermodynamic Studies on Oxidation and Desulphurization of Organic Sulphur from India Coal at 50-150°C. *Fuel. Processing Technology*. 2001;72(2):83-101
 37. Bruylant G, Wouters J, Michaux C. Differential Scanning Calorimetry in Life Science: Thermodynamics Stability, Molecular Recognition and Application in Drug Design. *Current Medicinal Chemistry*. 2005; 12: 2011-20.
 38. oshi K R, Rojivadiya A J, Pandya J H. Synthetic and Spectroscopic and Antimicrobial Studies of Schiff Base Metal Complexes Derived from 2-hydroxy-3- methoxy-5-nitrobenzaldehyde. *Int. Journal of Inorganic Chem*, 2014, 817412.
 39. Emara AAA, Ali AM, El-Asmy AF, Ragab EM. Investigation of the Oxygen Affinity of Manganese(II), Cobalt (II) and Nickel(II) Complexes with Some Tetradentate Schiff Bases. *Journal of Saudi Chemical Society*. 2011; 18 (6): 762-73.